



Physics-informed neural networks for simultaneous multi-anomaly inversion of self-potential data

Peter Adetokunbo^{1*}, Ayodeji Adekunle Eluyemi², Michael Ayuk Ayuk³

¹ Boone Pickens School of Geology, Oklahoma State University, Stillwater Oklahoma, USA

² Centre for Energy Research and Development (CERD), Obafemi Awolowo University (OAU), Ile Ife, Osun State, Nigeria

³ Department of Applied Geophysics, Federal University of Technology, Akure, Ondo State, Nigeria

Corresponding Author: Peter Adetokunbo¹

Abstract

Self-potential (SP) method represents a passive geophysical technique widely applied in mineral exploration, hydrogeophysics, and archaeological prospecting. Traditional interpretation approaches rely on derivative-based optimization methods that frequently encounter difficulties with parameter uniqueness, convergence to local minima, and sensitivity to noise contamination. This study presents a new approach which incorporates physics-informed neural network (PINN) framework for automated and simultaneous multi-anomaly quantitative interpretation. The PINN training objective employs a weighted multi-term loss function consisting of data misfit between neural network predictions and observed measurements, physics-informed residuals enforcing consistency with analytical forward models, and regularization constraints which prevents source position drift. PINN architecture embeds analytical forward models for various geometric sources including inclined sheets, spheres, and horizontal and vertical cylinders directly into the neural network training. Validation against published field data from the Baniyas archaeological site in Northern Israel demonstrates that the method recovers source parameters (depth, horizontal position of the center of anomaly) with deviations typically less than 5% from independent interpretations, while achieving root-mean-square errors of 0.018–0.038 mV. The framework successfully processes multiple anomalies simultaneously without requiring isolation procedures, addressing a critical limitation of existing interpretation methods. The complete methodology has been implemented as a publicly accessible web-based application, enabling researchers and practitioners worldwide to perform quantitative SP interpretation through an intuitive interface without requiring specialized programming expertise.

Keywords: Self-potential method, physics-informed neural networks, geophysical inversion, quantitative interpretation, multi-anomaly processing, deep learning

Introduction

The self-potential (SP) method is a non-invasive geophysical technique that measures naturally occurring electrical potentials to investigate subsurface features. These signals arise from various geological processes, including groundwater flow, electrochemical gradients along ore bodies, and thermal or hydrothermal activities (Revil *et al.*, 2017; Abdelrahman and Gobashy, 2021) ^[1, 17]. The method has found extensive applications across diverse fields, ranging from mineral exploration and hydrogeophysics to environmental monitoring and archaeological prospecting, due to its sensitivity to fluid movements through fractured and porous rock under natural or applied hydraulic gradients (Martínez-Pagán *et al.*, 2010; Adetokunbo *et al.*, 2024) ^[2, 14]. Estimation of model parameters in SP studies has traditionally faced substantial challenges, primarily due to the non-uniqueness of the inverse problem and sensitivity to noisy or incomplete field data (Göktürkler and Balkaya, 2012) ^[9]. The numerical challenges arise from the fact that multiple subsurface configurations can produce similar anomalies, leading to non-unique solutions. Traditional derivative-based methods require initial guesses close to the true solution and may converge to local minima rather than global optima, severely limiting their reliability in complex geological settings (Shaw and Srivastava, 2007; Durdağ *et al.*, 2022) ^[5, 18].

Recent advances in computational geophysics have explored metaheuristic optimization techniques including particle swarm optimization (PSO), genetic algorithms, and

differential evolution for SP data interpretation (Fernández-Martínez *et al.*, 2010 ^[8]; Lue *et al.*, 2024). While these approaches demonstrate superior global search capabilities compared to traditional methods, they often require extensive computational resources and lack the ability to incorporate physical constraints naturally into the optimization process.

The emergence of physics-informed neural networks (PINNs) represents a paradigm shift in scientific computing and inverse problems, offering the ability to combine data-driven learning with physics-based constraints (Raissi *et al.*, 2019) ^[15]. PINNs embed differential equations directly into the neural network loss function, ensuring that learned solutions respect fundamental physical laws while maintaining flexibility to fit complex data patterns (Karniadakis *et al.*, 2021) ^[4]. This approach has demonstrated remarkable success across diverse applications including fluid dynamics (Cai *et al.*, 2021), heat transfer (Shukla *et al.*, 2022) ^[4, 16], materials science (Hernandez *et al.*, 2021) ^[10], and seismic wave propagation (Song *et al.*, 2021; Rasht-Behesht *et al.*, 2022) ^[16, 20]. Recent extensions have incorporated PINNs into various geophysical contexts including seismic inversion (Waheed *et al.*, 2021) ^[20], groundwater flow modeling (Ali *et al.*, 2024) ^[3], and gravity data interpretation (Martin and Schaub, 2022) ^[13]. Despite these advances in related geophysical domains, the application of physics-informed neural networks to self-potential data interpretation remains largely unexplored, presenting a significant opportunity to

address longstanding challenges in automated quantitative analysis of electrokinetic anomalies.

This study presents a novel physics-informed neural network approach for Self-potential (SP) data inversion. The method incorporates a multi-component loss function combining data fitting, physics enforcement, and geometric constraints that automatically detect anomaly centers and prevent parameter drift. Through testing on field data, we demonstrate the effectiveness of this integrated approach in providing reliable, physically consistent parameter estimates.

Methodology

1. Forward Modeling

The forward modeling of self-potential (SP) anomalies involves calculating the theoretical electrical potential at the surface due to subsurface polarized bodies of various geometric shapes. The SP anomaly is generated by electric dipoles within the subsurface body, and the potential at any observation point depends on the geometry, orientation, and electrical properties of the source (El-Araby, 2004; Abdelrahman and Gobashy 2021) ^[1, 6]. A generalized mathematical formulation for SP anomalies caused by different geometric bodies can be expressed as:

$$V_f = K \cdot \frac{(x - x_0) \cdot \cos \alpha - h \sin \alpha}{[(x - x_0)^2 + h^2]^q}$$

where K represents the electric dipole moment, x_0 is the horizontal position of the body center, h is the depth parameter, α is the orientation angle, q is the shape factor that determines the geometric body type. The shape factor q controls the decay characteristics of the anomaly and varies according to the geometric configuration of the polarized source body. For a sphere, the shape factor $q = 3/2$, which reflects the three-dimensional nature of the source and produces the characteristic rapid decay associated with spherical bodies. For a vertical cylinder, $q = 0.5$, representing a two-dimensional source that extends infinitely in the vertical direction, such as vertical dikes, faults, or pipe-like structures. The slower decay rate reflects the extended geometry of the source. For a horizontal cylinder, $q = 1.0$, which corresponds to linear sources extending perpendicular to the profile direction, commonly used to model horizontal ore bodies, tunnels, or geological contacts (Fernández-Martínez *et al.*, 2010) ^[8]. For our PINN implementation, we implemented all the models including dipping sheet model ($q = 1.5$) which provides a versatile representation of common geological sources including ore bodies, fault zones, and geological contacts.

2. Physics-Informed Neural Network Architecture

The Physics-Informed Neural Network architecture consists of a feed-forward neural network that learns the mapping from spatial coordinates to self-potential values while enforcing consistency with analytical forward models. The network employs three hidden layers with 50 neurons each, using hyperbolic tangent activation functions to capture the non-linear behavior of SP anomalies. This architecture contains approximately 5,250 learnable parameters comprising weights and biases. The forward pass through the network follows the standard deep learning formulation:

$$f(x; \theta) = W_4 \sigma(W_3 \sigma(W_2 \sigma(W_1 x + b_1) + b_2) + b_3) + b_4$$

Where x is the input position coordinate along the survey profile, $f(x; \theta)$ is the output self-potential field at position x , θ represents all network parameters and σ denotes the tanh activation function, W and b are weight matrices and bias vectors for the layers.

The core strength lies in a composite loss function that simultaneously enforces data fitting, physics constraints, and automatic source positioning. The total loss function combines three components:

$$L_{Total} = L_{data} + \lambda_{physics} \times L_{physics} + \lambda_{constraint} \times L_{constraint}$$

The data loss term measures mean squared error between observed SP measurements and network predictions:

$$L_{data} = \frac{1}{N} \sum_i^N [V_{obs}(x_i) - f(x; \theta)]^2$$

Where N represents the number of observation points. The physics loss enforces consistency with theoretical forward models by comparing network predictions against it at collocation points distributed throughout the model domain:

$$L_{physics} = \frac{1}{M} \sum_j^M [f(x; \theta) - V_f(x_j; \varphi)]^2$$

Where M denotes collocation points, V_f represents the theoretical SP response computed using source parameters $\varphi = \{K, x_0, h, \alpha\}$, and $\lambda_{physics}$ controls the relative weight of physics enforcement. The constraint loss automatically detects the anomaly center by identifying the extremum of SP position and prevents source location drift through:

$$L_{constraint} = (x_0 - x_{0_target})^2$$

Where $x_{0_target} = \arg \min (V_{f_obs}(x))$ represents the automatically detected target source position. The training process employs the Adam optimizer to simultaneously update both neural network weights θ and physical source parameters φ . The algorithm begins by randomly initializing network parameters and detecting x_{0_target} from the minimum or maximum observed SP position, which then initializes the source location parameter. Each training epoch computes the data loss using observed measurements, generates collocation points for physics loss calculation, and evaluates the constraint loss based on the current source position estimate. The optimizer updates all parameters while enforcing physical bounds to ensure realistic values, specifically constraining depth $h > 0$, limiting intensity $|K| < 1000$, and restricting the dip angle α to 0-180 degrees. These constraints are applied after every gradient update to prevent parameter drift during optimization. Convergence typically occurs within 1,000-10,000 epochs, determined by monitoring total loss improvement over consecutive iterations.

The implementation uses carefully selected hyperparameters based on empirical testing. The physics weight $\lambda_{physics}$ provides low or high enforcement that allows flexible data fitting while maintaining physical consistency, whereas the

constraint weight $\lambda_{\text{constraint}}$ enforces strong adherence to the detected anomaly center position. The Adam optimizer employs a standard learning rate of 0.001, processing the complete dataset in each iteration. Numerical stability is maintained through Xavier initialization of network weights and automatic gradient clipping to prevent explosive gradients during backpropagation. The training process provides real-time monitoring of parameter evolution, demonstrating how the source position remains constrained near the target location while other parameters optimize to achieve optimal data fit.

Validation against Established SP Interpretation: Baniyas Archaeological Site Case Study

The efficacy of the proposed Physics-Informed Neural Network framework was evaluated using a published self-potential dataset from the Roman archaeological site of

Baniyas in Northern Israel (Eppelbaum, 2021) [7]. This site features ancient Roman limestone constructions, including cemetery structures and aqueduct components, providing an ideal benchmark with well-documented geological context and independent geophysical validation through complementary magnetic surveys. The SP measurements were acquired over a 1x1 meter grid following standard field protocols for archaeological investigations. Eppelbaum (2021) [7] interpretation identified two distinct self-potential anomalies within the survey area, each exhibiting characteristic signatures consistent with subsurface archaeological features. Figure 1 presents the digitized SP field map, clearly delineating the spatial distribution of both anomalies. A key advantage of the proposed PINN methodology is its inherent capability for simultaneous multi-anomaly analysis, as demonstrated in the multi-window analysis interface

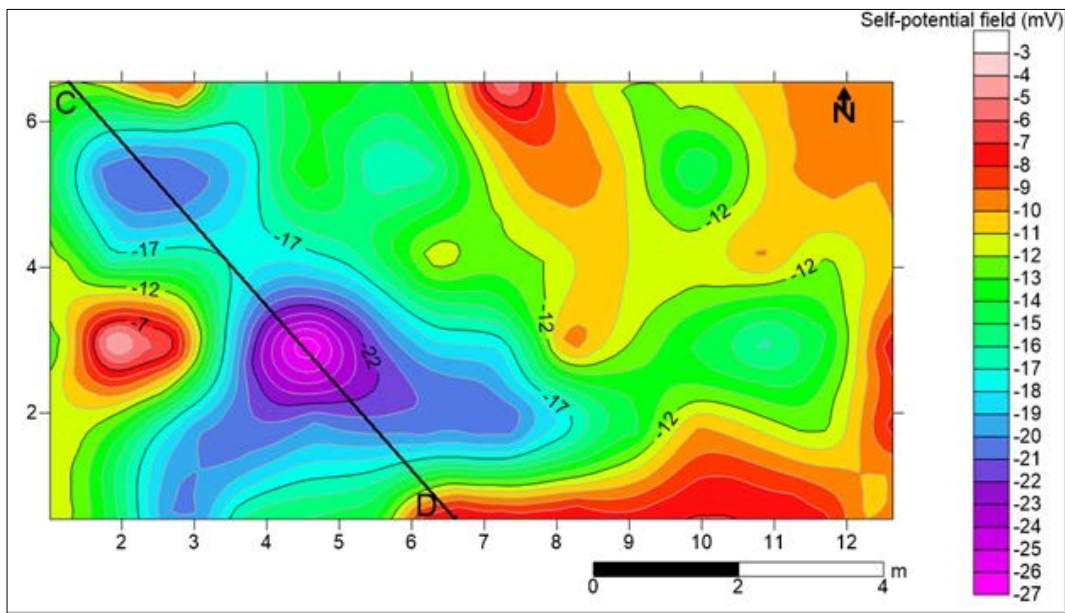


Fig 1: Digitize self-potential field map of Roman Site of Baniyas, Northern Israel and location of interpreting profiles CD (map reproduced from Eppelbaum, 2021) [7]

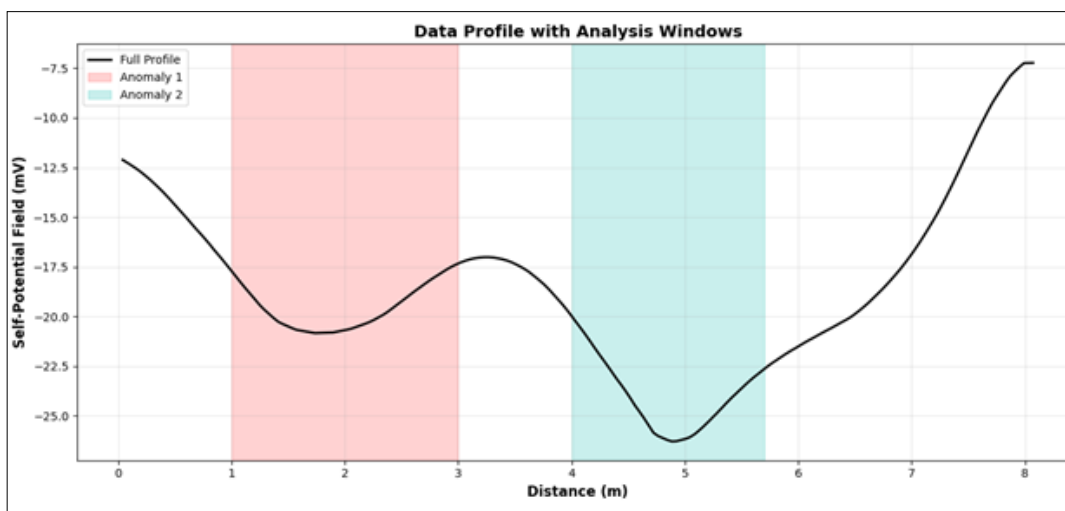


Fig 2: SP profile CD of the Baniyas site (northern Israel) which distinctively captured two anomalies highlighted in colors.

Shown in Figure 2. This concurrent processing approach eliminates the need for sequential anomaly isolation procedures commonly required in conventional interpretation workflows.

The first anomaly was interpreted using a horizontal circular cylinder (HCC) geometric model, consistent with the expected geometry of buried cylindrical archaeological structures such as ceramic pipes or column segments. Figure

3 illustrates the quantitative analysis of profile line CD for this feature. The PINN-derived synthetic SP response demonstrates excellent agreement with the observed field data, achieving a root-mean-square error of 0.038 mV. The inverted source parameters yield a depth estimate of $h = 1.66$ m and recover the anomaly center position. This depth estimation falls within the upper range of Eppelbaum (2021) [7] published values of 1.1–1.6 m, with the discrepancy potentially attributable to differences in geometric parameterization and regularization strategies between methodologies.

The second anomaly was characterized using an inclined thin sheet model, representative of thin planar archaeological features such as wall foundations or

pavement remnants. Figure 4 displays the quantitative interpretation results for this feature along the same profile. The PINN inversion achieved excellent data fit quality with an RMS error of only 0.018 mV, indicating superior model-data consistency. The recovered source parameters include a depth of $h = 1.46$ m and precise determination of the sheet horizontal center position. This depth estimate similarly aligns well with the reference interpretation, demonstrating the method's robustness across different geometric source configurations. Table 1 presents a comparison between the PINN-derived parameters and published values. The results demonstrate strong concordance across all recovered parameters, with depth estimates and horizontal positions typically exhibiting deviations of less than 5%. This

Table 1: Quantitative interpretation of self-potential anomalies along profile CD

Methods	Anomaly	Model	Center of Anomaly (X_0)	Depth to the Top of Anomaly (h)
PINN	Anomaly 1	HCC	1.75	1.66
Published Analytical	Anomaly 1	HCC	2.1	1.6
PINN	Anomaly 2	Inclined Sheet	4.89	1.46
Published Analytical	Anomaly 2	Thin Bed	5.1	1.2

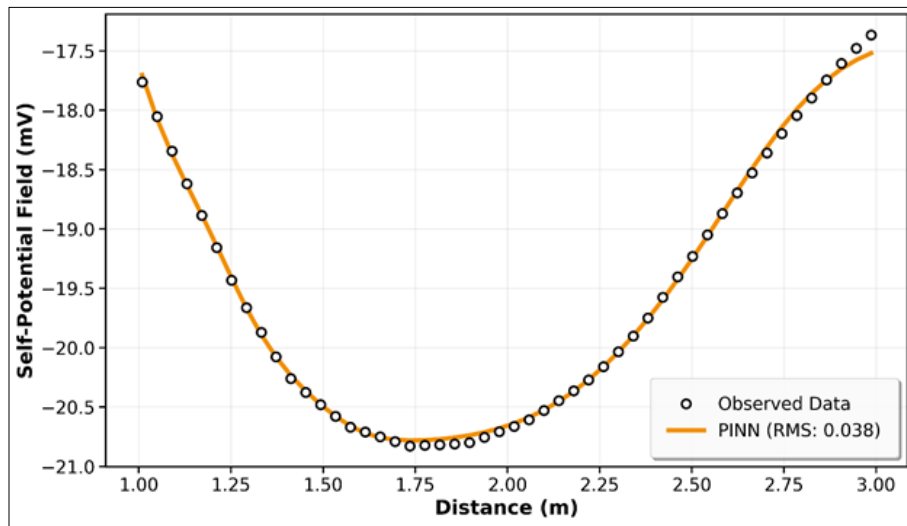


Fig 3: Quantitative analysis of SP anomaly 1 of the Baniyas site using horizontal cylindrical model

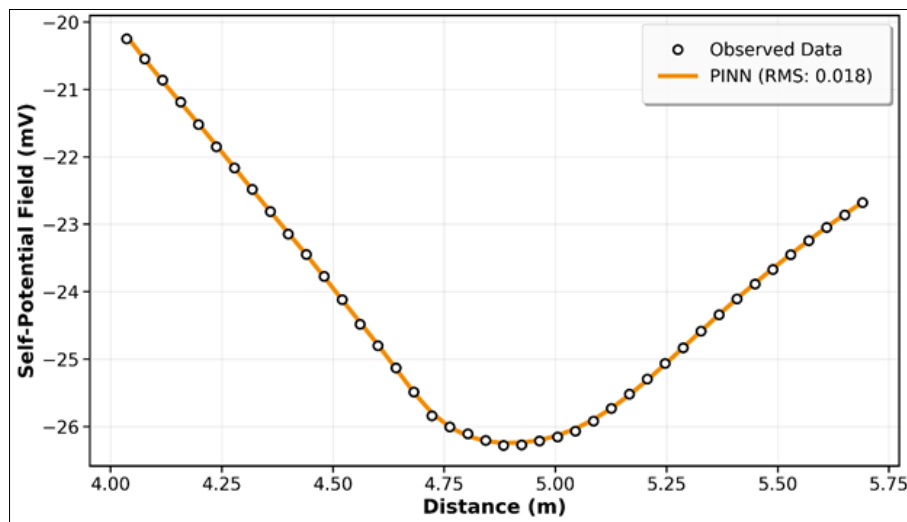


Fig 4: Quantitative analysis of SP anomaly 2 of the Baniyas site using inclined sheet model

Agreement validates the physical consistency and reliability of the PINN inversion framework for archaeological SP interpretation. It is noteworthy to know that the center of

anomalies do not exactly match those published simply because the profile direction is not the same. In the published data, 2 profile lines were drawn to capture the two

anomalies, whereas since PINN has capability of multi-anomaly processing, one profile line was drawn to capture the two anomalies, hence the difference in the estimation, however, the direction of profiling doesn't affect the depth of the causative body.

Discussion

The PINN algorithm demonstrates excellent capability in estimating source parameters from self-potential anomalies, as substantiated by the successful interpretation of the multi-anomaly Baniyas case study. The comparative analysis reveals that the proposed approach consistently produces parameter estimates in close agreement with independently published results. The depth and horizontal position estimates recovered by the PINN methodology exhibit excellent concordance with reference values, typically deviating by less than 5%. More significantly, the method demonstrates good stability when processing noise-contaminated data—a ubiquitous challenge in any geophysical field surveys. This robustness stems from the neural network's intrinsic capacity to learn noise-resistant data representations that preserve essential signal characteristics while attenuating measurement artifacts.

The versatility of the PINN framework becomes particularly evident when analyzing sources with diverse geometric configurations. For the horizontal circular cylinder and inclined thin sheet cases, the method successfully recovered source parameters.

Traditional derivative-based SP interpretation methods frequently encounter difficulties with parameter uniqueness, particularly when initial parameter estimates are poorly constrained or when data quality is marginal. Local minima in the objective function landscape can trap conventional optimizers, yielding geologically unrealistic or unstable solutions. The PINN approach circumvents these limitations through its stochastic gradient descent training process, combined with appropriate learning rate scheduling and batch processing strategies, which enables thorough exploration of the parameter space. The network progressively refines parameter estimates from coarse-scale global patterns to fine-scale local adjustments, effectively navigating complex objective function topographies.

The method scales efficiently to complex scenarios involving multiple simultaneous anomalies by expanding the source parameter vector while maintaining the core neural network architecture. The physics constraints and automatic positioning mechanisms extend naturally to multi-source configurations, providing a unified framework for interpreting composite SP signatures without requiring anomaly separation or sequential processing.

The successful implementation of simultaneous multiple anomaly processing addresses a longstanding limitation in SP interpretation methodology. Many conventional techniques require either anomaly isolation through filtering operations or sequential analysis of individual features, introducing potential artifacts and limiting interpretative flexibility. The PINN algorithm processes the entire dataset holistically, jointly inverting for all source parameters while respecting inter-source relationships and cumulative field effects. This holistic inversion capability proves particularly valuable in mineral exploration and archaeological prospecting, where multiple sources of varying geometry and strength commonly superpose. The Baniyas case study exemplifies this capability, demonstrating successful

recovery of parameters for two distinct anomalies of different geometric types within a single inversion run.

Field SP measurements invariably contain noise from diverse sources including telluric currents, electrochemical effects, temporal drift, and instrumentation limitations. Derivative-based interpretation methods can be severely compromised by such contamination, as numerical differentiation amplifies high-frequency noise components. The PINN approach exhibits inherent noise tolerance through its data-driven learning paradigm, which naturally filters noise while preserving diagnostic signal features. This advantage emerges from the regularization implicit in the neural network architecture and the multi-component loss function that balances data fidelity with physics consistency.

Several promising avenues exist for extending and enhancing the PINN methodology. Integration with complementary geophysical datasets to enhance interpretation, and incorporation of Bayesian neural network architectures or ensemble methods to provide uncertainty estimates for recovered parameters which will help to facilitate risk assessment and decision-making.

Conclusions

This study successfully developed and validated a physics-informed neural network framework for automated parameter estimation of self-potential anomalies, incorporating automatic source positioning constraints and multi-anomaly processing capabilities. The research demonstrates that integrating deep learning flexibility with rigorous geophysical forward modeling through multi-component loss functions yields a robust, efficient, and reliable approach to SP data interpretation that significantly advances current methodological standards. The successful integration of data fitting objectives with embedded geoelectric forward models ensures geologically realistic parameter estimates while maintaining superior data fit quality, leveraging neural network flexibility while respecting fundamental physical principles.

The demonstration of simultaneous multi-source inversion capabilities represents a significant advancement, as the method processes composite SP signatures holistically, eliminating the need for anomaly isolation procedures and enabling interpretation of geologically complex scenarios. Validation performance confirms that the method maintains parameter accuracy and stability under conditions that challenge conventional interpretation techniques. The achievement of convergence within practical timeframes of 2–5 minutes on standard computing hardware makes the methodology suitable for routine field data processing and near-real-time applications.

The physics-informed learning strategy effectively synthesizes the complementary strengths of neural networks and traditional geophysical modeling. Neural networks provide flexible, data-driven approximation capabilities that can accommodate complex noise patterns and non-linear parameter relationships, while forward modeling embeds domain-specific physical knowledge that constrains the solution space to geophysically plausible parameter combinations. The validation against published field data from the Baniyas archaeological site confirms that the PINN methodology recovers source parameters consistent with independent interpretations while offering enhanced automation, robustness, and multi-anomaly processing capabilities.

The demonstrated capabilities have immediate practical relevance across multiple application domains including archaeological prospection for rapid, objective interpretation of SP signatures from buried structures; mineral exploration for automated delineation of ore body geometry and depth in complex multi-source environments; hydrogeophysics for characterization of subsurface fluid flow pathways and contaminant plume geometry; and engineering site investigation for assessment of foundation conditions and identification of subsurface voids or heterogeneities. Future research should prioritize extension to three-dimensional coupled inversion, development of joint multi-physics inversion capabilities, implementation of Bayesian uncertainty quantification, and creation of real-time processing systems for continuous monitoring applications.

References

1. Abdelrahman ESM, Gobashy MM. A fast method for interpretation of self-potential anomalies due to buried bodies of simple geometry. *Pure and Applied Geophysics*,2021:178(8):3027-3038. <https://doi.org/10.1007/s00024-021-02858-5>
2. Adetokunbo P, Ismail A, Mewafy F, Sanuade O. Geophysical characterization and seepage detection of the Chimney Rock Dam embankment near Salina, Oklahoma. *Water*,2024:16(9):1224. <https://doi.org/10.3390/w16091224>
3. Ali ASA, Jazaei F, Clement TP, Waldron B. Physics-informed neural networks in groundwater flow modeling: Advantages and future directions. *Groundwater for Sustainable Development*,2024:25:101172. <https://doi.org/10.1016/j.gsd.2024.101172>
4. Cai S, Mao Z, Wang Z, Yin M, Karniadakis GE. Physics-informed neural networks (PINNs) for fluid mechanics: A review. *Acta Mechanica Sinica*,2021:37(12):1727-1738. <https://doi.org/10.1007/s10409-021-01148-1>
5. Durdağ D, Ayhan Durdağ G, Pekşen E. Inversion of self-potential data using generalized regression neural network. *Acta Geodaetica et Geophysica*,2022:57(4):589-608. <https://doi.org/10.1007/s40328-022-00396-2>
6. El-Araby HM. A new method for complete quantitative interpretation of self-potential anomalies. *Journal of Applied Geophysics*,2004:55(3-4):211-224. <https://doi.org/10.1016/j.jappgeo.2003.11.002>
7. Eppelbaum LV. Review of processing and interpretation of self-potential anomalies: Transfer of methodologies developed in magnetic prospecting. *Geosciences*,2021:11(5):194. <https://doi.org/10.3390/geosciences11050194>
8. Fernández-Martínez JL, García-Gonzalo E, Fernández-Álvarez JP, Kuzma HA, Menéndez CO. PSO: A powerful algorithm to solve geophysical inverse problems: Application to a 1D-DC resistivity case. *Journal of Applied Geophysics*,2010:71(1):13-25. <https://doi.org/10.1016/j.jappgeo.2010.02.001>
9. Göktürkler G, Balkaya Ç. Inversion of self-potential anomalies caused by simple-geometry bodies using global optimization algorithms. *Journal of Geophysics and Engineering*,2012:9(5):498-507. <https://doi.org/10.1088/1742-2132/9/5/498>
10. Hernandez Q, Badias A, González D, Chinesta F, Cueto E. Structure-preserving neural networks. *Journal of Computational Physics*,2021:426:109950. <https://doi.org/10.1016/j.jcp.2020.109950>
11. Karniadakis GE, Kevrekidis IG, Lu L, Perdikaris P, Wang S, Yang L. Physics-informed machine learning. *Nature Reviews Physics*,2021:3(6):422-440. <https://doi.org/10.1038/s42254-021-00314-5>
12. Luo Y, Du X, Cui Y, Guo Y, Xie J, Liu J. Inversion of self-potential source based on particle swarm optimization. *Geophysical Prospecting*,2023:71(2):322-335. <https://doi.org/10.1111/1365-2478.13299>
13. Martin J, Schaub H. Physics-informed neural networks for gravity field modeling of small bodies. *Celestial Mechanics and Dynamical Astronomy*,2022:134:46. <https://doi.org/10.1007/s10569-022-10101-8>
14. Martínez-Pagán P, Gomez-Ortiz D, Martín-Crespo T, Manteca JI, Ovejero G. The electrical resistivity tomography method in the detection of shallow mining cavities. A case study on the Victoria Cave, Cartagena (SE Spain). *Engineering Geology*,2010:114(1-2):1-12. <https://doi.org/10.1016/j.enggeo.2013.01.013>
15. Raissi M, Perdikaris P, Karniadakis GE. Physics-informed neural networks: A deep learning framework for solving forward and inverse problems involving nonlinear partial differential equations. *Journal of Computational Physics*,2019:378:686-707. <https://doi.org/10.1016/j.jcp.2018.10.045>
16. Rasht-Behesht M, Huber C, Shukla K, Karniadakis GE. Physics-informed neural networks (PINNs) for wave propagation and full waveform inversions. *Journal of Geophysical Research: Solid Earth*,2022:127(5):e2021JB023120. <https://doi.org/10.1029/2021JB023120>
17. Revil A, Coperey A, Shao Z, Florsch N, Fabricius IL, Deng Y, *et al.* Complex conductivity of soils. *Water Resources Research*,2017:53:7121-7147. <https://doi.org/10.1002/2017WR020655>
18. Shaw R, Srivastava S. Particle swarm optimization: A new tool to invert geophysical data. *Geophysics*,2007:72(2):F75-F83. <https://doi.org/10.1190/1.2432481>
19. Shukla K, Xu M, Trask N, Karniadakis GE. Scalable algorithms for physics-informed neural and graph networks. *Data-Centric Engineering*,2022:2:e24. <https://doi.org/10.1017/dce.2021.24>
20. Song C, Alkhalifah T, Waheed UB. Solving the frequency-domain acoustic VTI wave equation using physics-informed neural networks. *Geophysical Journal International*,2021:225(2):846-859. <https://doi.org/10.1093/gji/ggab010>
21. Waheed UB, Alkhalifah T, Haghghat E, Song C, Hao Q. PINNeik: Eikonal solution using physics-informed neural networks. *Computers & Geosciences*,2021:155:104833. <https://doi.org/10.1016/j.cageo.2021.104833>